Article

Lamellar Stacking Split by In-Membrane Clustering of Bulky Glycolipids

E. Del Favero, A. Raudino, P. Brocca, S. Motta, G. Fragneto, M. Corti, and L. Cantú

Langmuir, **2009**, 25 (7), 4190-4197• DOI: 10.1021/la802858m • Publication Date (Web): 24 December 2008

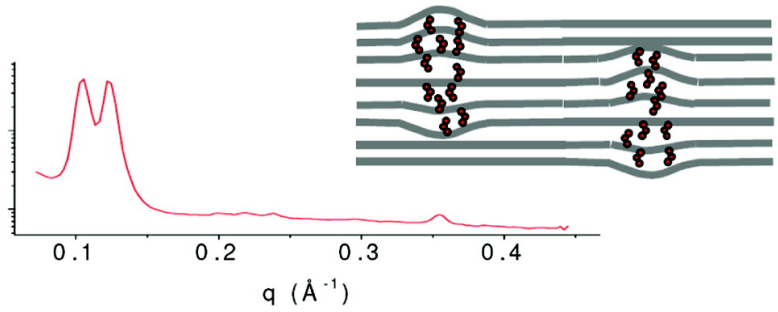

More About This Article

Additional resources and features associated with this article are available within the HTML version:

- Supporting Information
- Access to high resolution figures
- Links to articles and content related to this article
- Copyright permission to reproduce figures and/or text from this article

View the Full Text HTML

Lamellar Stacking Split by In-Membrane Clustering of Bulky Glycolipids†

E. Del Favero,‡ A. Raudino,*,§ P. Brocca,‡ S. Motta,‡ G. Fragneto,|| M. Corti,‡ and L. Cantú‡

Department of Medical Chemistry, Biochemistry and Biotechnologies, University of Milan, L.I.T.A., Via F. lli Cervi 93, 20090 Segrate, Italy, Department of Chemical Science, University of Catania, Viale A. Doria 6, 95125, Catania, Italy, and Institut Laue-Langevin, 6 rue Jules Horowitz, BP 156, 38042 Grenoble Cedex 9

Received September 1, 2008. Revised Manuscript Received November 13, 2008

We developed a simple model to investigate the effect of lipid clustering on the local interlayer distance in a cluster of interacting lamellae. The model, based on nonequilibrium thermodynamics and linear stability theories, explores the early stages of the lamella−lamella phase separation process where the lateral diffusion is much faster than the interlamellar lipid exchange. Results indicate, in the early stages, the presence of locally distorted regions with a higher concentration of one lipid component and an anomalous repeat distance. Experimental cases are presented, consisting of multilamellar-oriented depositions of phospholipids containing minority amounts of ganglioside or sphingomyelin under a low-hydration condition. The minority components are known to form domains within the phospholipid bilayer matrix. The low water content inhibits the lipid exchange among nearby lamellae and strengthens lamella−lamella interaction, allowing for a straightforward comparison with the model. Small-angle and wide-angle neutron diffraction experiments were performed in order to detect interlayer distances and local chain order, respectively. Lamellar stacking splitting has been observed for the ganglioside-containing lamellae, induced by in-phase lipid clustering. In excess water and after long equilibration times, these local structures may further evolve, leading to coexisting lamellar phases with different lipid compositions and interlayer distances.

1. Introduction

The formation and morphology of microdomains with nonaverage composition in multicomponent systems has been very actively addressed in fundamental and applied research. A customary theoretical approach is the so-called spinodal decomposition theory proposed by Cahn and Hilliard[1] in the mid-1960s and further developed by several authors. Nowadays, related theories are routinely applied to explore a variety of systems, ranging from metal alloys,[2] polymer blends,[3] liquid crystals,[4] dewetting processes,[5] and the formation of microdomains in multicomponent cell membranes,[6,7] just to quote a few examples.

In the spinodal decomposition models, the amplitude of the compositional fluctuations generated by a sudden disturbance of any relevant physical variable exponentially grows with time until mesoscopic phase-separation occurs. Not all of the fluctuations, however, grow at the same rate, and the fastest growing fluctuations determine the final morphology of the sample.

Let us turn our attention to the formation of domains inside an array of multicomponent closely packed soft lamellae (lipid membranes). Any localized compositional changes affect the interlamellar repulsion, thus the system exhibits strong coupling between the local composition and the interlamellar repeat distance, which may not remain constant because of localized compression of the lamellae. Besides the evident biological interest, this problem is particularly attractive because of the involved different time scales. Consider first the long-time response to a sudden variation in any physical parameter. The system behaves as a strong anisotropic fluid, where the individual lipids may transfer themselves from one lamella to another. Such a system may phase separate into an array of A-rich and B-rich lamellae having different interactions and therefore different spacing. This process requires long equilibration times because of the slow interlamellar transfer rate of the lipids in comparison with the fast lipid motion within a single lamella.[8] A cartoon of the above-described macroscopic phase separation in an array of two-componentrigid bilayers is shown in Figure 1 (panel A).

From an experimental point of view, the lamellar−lamellar phase coexistence in self-assembled systems of amphiphilic molecules is well established. In several systems, higher-density (condensed) lamellar phases in thermodynamic equilibrium with low-density (swollen) lamellar phases have been observed. Such an effect has been mainly found in ternary systems involving two amphiphilic molecules and water, like mixtures of two different zwitterionic phosphatidylcholines in the presence of calcium ions,[9,10] mixtures of sodium octanoate and octylammonium octanoate,[11] and aqueous mixtures of anionic and cationic

† Part of the Neutron Reflectivity special issue.

* Corresponding author. E-mail: araudino@dipchi.unict.it. Tel: ++39 0957385078.

‡ University of Milan.

§ University of Catania.

|| Institut Laue-Langevin.

(1) Cahn, J. W. *J. Chem. Phys.* **1965**, *42*, 93.

(2) Porter, D. A.; Easterling, K. E. *Phase Transformations in Metals and Alloys*; CRC Press: Boca Raton, FL, 1992.

(3) Binder, K. *J. Chem. Phys.* **1983**, *79*, 6387.

(4) Dhont, J. K. G.; Briels, W. J. *Phys. Rev. E* **2005**, *72*, 031404.

(5) Sharma, A.; Khanna, R *Phys. Rev. Lett.* **1998**, *81*, 3463.

(6) Gelbart, W. A.; Bruinsma, R. *Phys. Rev. E* **1997**, *55*, 831.

(7) Nielsen, L. K.; Vishnyakov, A.; Jorgensen, K.; Bjornholm, T.; Mouritsen, O. G. *J. Phys.: Condens. Matter* **2000**, *12*, A309.

(8) Cevc, G.; Marsh, D. *Phospholipid Bilayers*; Wiley: New York, 1985.

(9) Lis, L. J.; Parsegian, V. A.; Rand, R. P. *Biochemistry* **1981**, *20*, 1761.

(10) Lis, L. J.; Lis, T.; Parsegian, V. A.; Rand, R. P. *Biochemistry* **1981**, *20*, 1771.

(11) Jokela, P.; Jonsson, B.; Eichmuller, B.; Fontell, K. *Langmuir* **1988**, *4*, 187.

10.1021/la802858m CCC: $40.75
Published on Web 12/24/2008

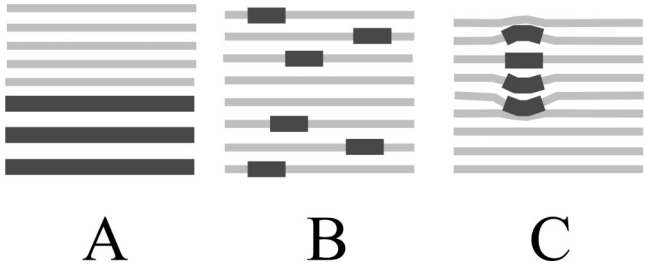

Figure 1. (A) Schematic drawing of a macroscopically phase-separated array of two-component rigid lamellae. (B) Lipid lamellae. Cluster formation of one-component-rich domains within the individual lamellae, with random 3D cluster arrangement. (C) Lipid lamellae. Possible effect on the local interlamellar spacing, producing regions with a larger or smaller interlamellar distance, induced by in-phase lipid clustering.

surfactants.[12] In a few cases, the lamella−lamella coexistence has also been observed in binary water/surfactant systems.[13−15] Equilibrium calculations of mixed lamellar systems have been performed.[16−18] They evidence a macroscopic phase separation where condensed lamellar phases are in thermodynamic equilibrium with a swollen lamellar phase.

In this article, we focus on the development of a model predicting the short-time behavior of a lipid stack of lipid lamellae following a perturbation of any relevant variable. The starting point is that, at short times, interlamellar lipid exchange is prevented but the lateral lipid redistribution inside the lamellar plane is retained. As a result of an applied perturbation, the mixing entropy can be overrun by the interactions among the lipids, inducing the formation of local domains richer in a specific component. If these localized domains exhibit a stronger interlamellar repulsion/attraction, then it is likely due to the formation of local patches with a different interlamellar distance. This process, however, requires an energetically expensive bending deformation of the lamellae at the boundary between A-rich and B-rich domains in order to support a different interlamellar spacing while moving along the membrane plane. For rigid bilayers with a high bending constant, it is then evident, from the above considerations, that domain formation is not favored in the short-time limit because the lipid lateral rediffusion of the individual lamellae relieves in part the unfavorable repulsion and the lamellar bending deformation energy. Therefore, no peculiar short-time behavior is likely to be observed in phase-separated stacks of rigid lamellae as the system approaches the long-time configuration.

A different situation may occur in the case of soft lamellae, such as lipid bilayers, with a bending elasticity modulus in the range of (1−50)*kT*. (For a review, see ref 19). There, cluster formation can occur, as sketched in Figure 1B, for one-component-rich domains within the individual lamellae. Lipid clustering introduces localized repulsions and/or attraction among the soft lamellae. Lipid clustering can, in addition, modulate the local interlamellar spacing, producing regions with larger or smaller interlamellar distance with respect to the homogeneous case (Figure 1C).

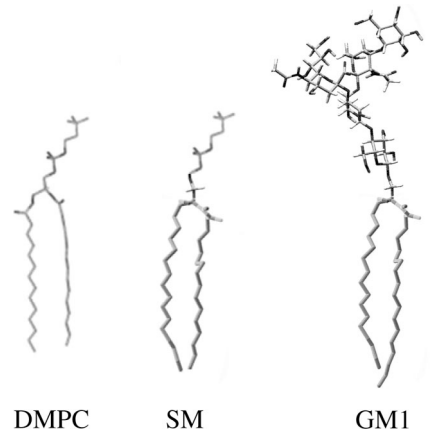

Figure 2. Structures of dimyristoylphosphatidylcholine (DMPC), palmitoyl sphingomyelin (SM), and ganglioside GM1.

To investigate experimentally the above-described structures occurring in the early stage of the lamella−lamella phase-separation process, we performed small-angle and wide-angle neutron diffraction measurements in multistacks of mixed lamellae at low water content. In particular, highly oriented depositions constituted of phospholipid DMPC mixed with a minor amount of ganglioside GM1 or sphingomyelin have being investigated. Figure 2 reports the structures of the different lipids. The low molar fraction of the second components, very far from the half-proportion, guarantees high miscibility and prevents macroscopic phase separation. On the other side, sphingolipids, both GM1 and sphingomyelin, show a pronounced tendency to form enriched domains within both natural and artificial membranes.[20] Furthermore, all of the considered amphiphiles have long residence times (very low cmc's) that ensures negligible interlamellar lipid redistribution, making short times very long on an absolute time scale. The low water content allows for extensive short-range interlamellar interactions. In addition, looking at the biological side of the problem, this short-time behavior is of particular interest if related to real membranes. In fact, it is claimed that important physiological processes, such as cell-to-cell adhesion, are mediated by glycosphingolipid-enriched microdomains interfacing between two adjacent cells, requiring stabilization against the lipid redistribution of similar domains sitting on different membranes coming into contact, on short times. The proposed model sketches in simple terms the possible local structural response to a domain−domain interaction taking place between close facing membranes, before specific physical and biological events take place.

2. Model

Consider a cluster of N lipid bilayers separated by water sheets of mean thickness a. We assume that the bilayers are formed by different lipids, where the concentration of each jth component in a generic sth bilayer is denoted as C_s^j. We assume that the bilayers are either in a pure fluid or in a pure gel phase, whereas no coexistence of gel and fluid domains is allowed. Such a condition is easily met at temperatures far from the gel−fluid transition temperature T_m. Close to T_m, an additional variable p_s^j describing the order parameter of the lipid hydrocarbon tails must be considered, making the local composition and the lipid tails order two strongly coupled properties (see, e.g., ref 7). In the following text, we neglect the coupling between p_s^j and C_s^j by assuming a constant order parameter.

(12) Marques, E.; Khan, A.; daGraca Miguel, M.; Lindman, B. *J. Phys. Chem.* **1993**, *97*, 4729.
(13) Dubois, M.; Zemb, T.; Belloni, L. *J. Chem. Phys.* **1992**, *96*, 2278.
(14) Dubois, M.; Zemb, T.; Fuller, N.; Rand, R. P.; Parsegian, V. A. *J. Chem. Phys.* **1998**, *108*, 7855.
(15) Cantù, L.; Corti, M.; Del Favero, E.; Raudino, A. *Langmuir* **2000**, *16*, 8903.
(16) Leibler, S.; Andelman, D. *J. Phys. (Paris)* **1987**, *48*, 2013.
(17) Noro, M. G.; Gelbart, W. M. *J. Chem. Phys.* **1999**, *111*, 3733.
(18) Harries, D.; Podgornik, R.; Parsegian, V. A.; Mar-Or, E.; Andelman, D. *J. Chem. Phys.* **2006**, *124*, 224702.
(19) Seifert, U.; Lipowsky R. In *Handbook of Biological Physics*; Lipowsky, R., Sackmann, E., Eds.; Elsevier: Amsterdam, 1995; Vol.1, p 403.
(20) Masserini, M.; Ravasi, D. *Biochim. Biophys. Acta* **2001**, *1532*, 149.

The total energy is partitioned into the sum of three contributions: (a) the self-energy of the isolated bilayers; (b) the interaction between each bilayer and its nearest neighbors; and (c) an elastic bending energy term accounting for the bilayer local deformation from their own planar shape

$$U_{\mathrm{TOT}} = U_{\mathrm{SELF}} + U_{\mathrm{INT}} + U_{\mathrm{ELASTIC}} \quad (1)$$

First we calculate the interaction term. Without a loss of generality, we set

$$U_{\mathrm{INT}} = \frac{1}{2}\sum_{j}\sum_{j'}\sum_{s=1}^{N}\int_S (C_s^j C_{s,s+1}^{j'} G_{jj'}(H_s - H_{s+1}) + C_s^j C_{s-1}^{j'} G_{jj'}(H_s - H_{s-1}))\,\mathrm{d}x\,\mathrm{d}y \quad (2)$$

which describes the interactions between j and j' molecules belonging to nearby bilayers. The integration is extended over the whole lamellar surface S, and the sum over s spans over all of the N lipid layers. The pair interaction energy $G_{jj'}(H_s - H_{s\pm1})$ is a function of the interlamellar distance $H_s - H_{s\pm1}$. It is useful to introduce the local deviation h_s from the interlamellar equilibrium distance a

$$H_s - H_{s\pm1} = a + (h_s - h_{s\pm1}) \quad (3a)$$

Analogously, we partition the local concentration C_s^j of the jth component as the sum of the mean concentration $\bar{C}^j$(independent of s) plus a local deviation, c_s^j, from the mean value

$$C_s^j = \bar{C}^j + c_s^j \quad (3b)$$

Clearly, the concentration fluctuations inside each bilayer, integrated over the whole bilayer surface S, must satisfy the mass conservation constraint

$$\int_S c_s^j\,\mathrm{d}S = 0 \quad (4)$$

The pair interaction energy $G_{jj'}(H_s - H_{s\pm1})$ is generally repulsive because of the overwhelming electrostatic and hydration forces with respect to the attractive dispersion term. To stabilize the layered structure, the repulsive forces must be balanced by an external pressure. The simplest way to describe the effect of the balancing pressure is that of imposing a constant volume on the water layers: $\sum_{s=1}^{N}\int_S {}^1/_2((H_s - H_{s+1}) + (H_s - H_{s-1}))\,\mathrm{d}S = Na^*S$, where the integrand being the mean thickness of a water layer around a generic sth lipid bilayer and a^* is the optimum interbilayer thickness. From the above relationship, we get $a = a^*$ and

$$\sum_{s=1}^{N}\int_S (2h_s - h_{s+1} - h_{s-1})\,\mathrm{d}S = 0 \quad (5)$$

Geometrical constraints impose a simple expression to a^* in a layered water−lamellae sample

$$a^* = L\frac{1-\Theta_{\mathrm{L}}}{\Theta_{\mathrm{L}}} \quad (6)$$

Θ_{L} is the lipid volume fraction in the lipid + water system, and L is the bilayer thickness (assumed to be incompressible).

Let us apply the previous equations to the simple case of a two-component bilayer (namely, $j, j' = \mathrm{A}$ or B). Let $\bar{C}^{\mathrm{A}} \equiv X$ and $\bar{C}^{\mathrm{B}} \equiv 1 - X$ be the mean concentrations of the A and B components, and let $c_s{}^{\mathrm{A}} = -c_s{}^{\mathrm{B}} \equiv \Phi_s$ be the corresponding concentration fluctuations around the mean value, expanding the interlamellar potential $G_{jj'}(H_s - H_{s\pm1})$ around the equilibrium distance $a = a^*$ that we obtain in the quadratic approximation

$$G_{jj'}(H_s - H_{s\pm1}) \approx G_{jj'}(a) + \frac{\partial G_{jj'}(a)}{\partial a}(h_s - h_{s\pm1}) + \frac{1}{2}\frac{\partial^2 G_{jj'}(a)}{\partial a^2}(h_s - h_{s\pm1})^2 \quad (7)$$

and, making use of the mass conservation (eq 4) and constant volume (eq 5) constraints to eliminate linear terms, we find

$$U_{\mathrm{INT}} = \mathrm{const} + \frac{1}{4}\sum_{s=1}^{N}\int_S [F_{XX}\Phi_s(\Phi_{s+1} + \Phi_{s-1}) + F_{aa}((h_s - h_{s+1})^2 + (h_s - h_{s-1})^2) + F_{aX}(\Phi_s(2h_s - h_{s+1} - h_{s-1}) + \Phi_{s+1}(h_s - h_{s+1}) + \Phi_{s-1}(h_s - h_{s-1}))]\,\mathrm{d}S \quad (8)$$

where the shorthand notation has been used: $F_{XX} \equiv \rho(\partial^2 F)/(\partial X^2)$, $F_{aa} \equiv \rho(\partial^2 F)/(\partial a^2)$, and $F_{aX} \equiv \rho(\partial^2 F)/(\partial X \partial a)$. The function $F \equiv F(X, a)$ is the interbilayer energy in the planar limit

$$F \equiv X^2 G_{\mathrm{AA}}(a) + 2X(1-X)G_{\mathrm{AB}}(a) + (1-X)^2 G_{\mathrm{BB}}(a) \quad (9)$$

An interesting feature of eq 8 is that the composition and spacing fluctuations are strongly coupled.

As shown in eq 1, the energy of interaction must be supplemented by the composition-dependent bilayers' self-energy. Following standard partitioning into an entropic and an interaction term for a heterogeneous distribution of close-packed particles, we write

$$U_{\mathrm{SELF}} = \sum_{s=1}^{N}\int_S \left[kT\sum_j C_s^j(r)\log C_s^j(r) + \frac{1}{2}\sum_j\sum_{j'}\int_S C_s^j(\vec{r})\, C_s^{j'}(\vec{r'})\, E_{ss}(|\vec{r} - \vec{r'}|)\,\mathrm{d}S'\right]\mathrm{d}S \quad (10)$$

The first term describes the mixing entropy, and the second term takes into account the pair interactions among lipids belonging to the same bilayer. Expanding $C_s^{j'}(\vec{r'})$ around $\vec{r}$, integrating over dS′, and using the mass conservation constraint (eq 5), we obtain for a two-component bilayer

$$U_{\mathrm{SELF}} = \mathrm{const} + \frac{1}{2}\sum_{s=1}^{N}\int_S \left[b((T - T_{\mathrm{C}}^{(\mathrm{o})})\Phi_s^2 + \kappa\left(\left(\frac{\partial\Phi_s}{\partial x}\right)^2 + \left(\frac{\partial\Phi_s}{\partial y}\right)^2\right)\right)\mathrm{d}S \quad (11)$$

where $T_{\mathrm{C}}{}^{(\mathrm{o})}$ is the critical temperature of the isolated membrane: $b((T - T_{\mathrm{C}}{}^{(\mathrm{o})}) \equiv \rho((kT)/(X(1-X)) - w_{||})$, $w_{||}$ is the preferential interaction parameters among lipids belonging to the same membrane, and $\kappa > 0$ (roughly proportional to $w_{||}$) is a measure of the resistance to the formation of concentration gradients in the membrane plane.

Finally, the elastic energy term can be written in the Helfrich approximation[21] as

$$U_{\mathrm{ELASTIC}} = \sum_{s=1}^{N}\int_S \left[\frac{1}{2}K_{\mathrm{M}}(\nabla^2 h_s)^2 - K_{\mathrm{G}}\left(\left(\frac{\partial^2 h_s}{\partial x^2}\right)\left(\frac{\partial^2 h_s}{\partial y^2}\right) - \left(\frac{\partial^2 h_s}{\partial x\,\partial y}\right)^2\right)\right]\mathrm{d}S \quad (12)$$

$\nabla^2 \equiv (\partial^2)/(\partial x^2) + (\partial^2)/(\partial y^2)$, where $K_{\mathrm{M}} \equiv K_{\mathrm{M}}(X)$ and $K_{\mathrm{G}} \equiv K_{\mathrm{G}}(X)$ are the bending rigidity and the Gaussian curvature modulus, respectively.

(21) Safran, S. A. *Statistical Mechanics of Surfaces, Interfaces and Membranes*; Addison-Wesley: Reading MA, 1994.

Adding together the different contributions, eqs 8, 11 and 12, we obtain the total free energy

$$U_{TOT} \equiv \text{const} + \frac{1}{2}\sum_{s=1}^{N}\int_S [K_M(\nabla^2 h_s)^2 - 2K_G\left(\left(\frac{\partial^2 h_s}{\partial x^2}\right)\left(\frac{\partial^2 h_s}{\partial y^2}\right) - \left(\frac{\partial^2 h_s}{\partial x\,\partial y}\right)^2\right) + \kappa\left(\left(\frac{\partial \Phi_s}{\partial x}\right)^2 + \left(\frac{\partial \Phi_s}{\partial y}\right)^2\right) + b(T - T_C^{(o)})\Phi_s^2 + \frac{1}{2}F_{XX}\Phi_s(\Phi_{s+1} + \Phi_{s-1}) + \frac{1}{2}F_{aa}((h_s - h_{s+1})^2 + (h_s - h_{s-1})^2) + \frac{1}{2}F_{aX}(\Phi_s(2h_s - h_{s+1} - h_{s-1}) + \Phi_{s+1}(h_s - h_{s+1}) + \Phi_{s-1}(h_s - h_{s-1}))]dS \quad (13)$$

To proceed further, we assume that the bilayer deformation h_s is always in equilibrium with the instantaneous local composition Φ_s of the bilayers. In other words, for a given Φ_s, the calculated h_s values are those corresponding to an energy minimum. A minimization procedure with respect to h_s and its higher-order derivatives leads to the Euler−Lagrange equation[22]

$$\frac{\delta U_{TOT}}{\delta h_s} = \frac{\partial U_{TOT}}{\partial h_s} - \sum_k \frac{\partial}{\partial x_k}\frac{\partial U_{TOT}}{\partial(\partial h_s/\partial x_k)} + \sum_k\sum_{k'}\frac{\partial^2}{\partial x_k\,\partial x_{k'}}\frac{\partial U_{TOT}}{\partial(\partial^2 h_s/\partial x_k\,\partial x_{k'})} = 0 \quad (14)$$

with $x_k = x,y$. Inserting the total energy (13) into eq. (14) we find

$$K_M\nabla^2\nabla^2 h_s + \frac{1}{2}F_{aa}(2h_s - h_{s+1} - h_{s-1}) + \frac{1}{4}F_{aX}(2\Phi_s + \Phi_{s+1} + \Phi_{s-1}) = 0 \quad (15)$$

where $\nabla^2\nabla^2 = (\partial^4)/(\partial x^4) + 2(\partial^4)/(\partial x^2\partial y^2) + (\partial^4)/(\partial y^4)$. Equation 15 enables one to calculate the coupling between distance and concentration fluctuations in multicomponent interacting lamellae. It is worth mentioning that the coupling does not depend any longer on the Gaussian curvature modulus K_G. For a system without composition fluctuations, $\Phi_s = 0$, and eq 15 reduces to the well-known expression for a cluster of identical oscillating lamellae.

In a nonequilibrium thermodynamics picture, the flux of lipids along the three Cartesian axes is proportional to the chemical potential gradient of the considered specie. Because we are investigating a two-component lipid mixture, only a single-compositional variable is required, thus

$$J_{s,x} = -M\frac{d\mu_s}{dx},\ J_{s,y} = -M\frac{d\mu_s}{dy},\ J_{s,z} = 0 \quad (16)$$

where M is a mobility coefficient in the membrane plane and the chemical potential μ_s is the functional derivative of the total free energy with respect to the local concentration Φ_s

$$\mu_s = \frac{\delta U_{TOT}}{\delta \Phi_s} \quad (17)$$

with the functional derivative being defined by eq 14. The first two equations for $J_{s,x}$ and $J_{s,y}$ describe the lipid motion along the membrane plane, and the third one accounts for the perpendicular transfer of lipids across different lamellae. Lipid exchange among bilayers separated by water sheets is much slower than the lateral motions in the same bilayer;[8] for this reason, we imposed $J_{s,z} = 0$. Such an assumption is incorrect in a time-independent model, but it is reasonable when processes with time scales shorter than the lipid transfer among different lamellae are considered. The fluxes defined by eq 16 must satisfy the 2D continuity equation

$$-\frac{\partial \Phi_s}{\partial t} = \frac{\partial J_{s,x}}{\partial x} + \frac{\partial J_{s,y}}{\partial y} \quad (18)$$

which, combined with the previous equations, yields, after straightforward algebra,

$$\frac{\partial \Phi_s}{\partial t} = M\nabla^2\left[-\kappa\nabla^2\Phi_s + \tau_o\Phi_s + \frac{1}{4}F_{XX}(\Phi_{s+1} + \Phi_{s-1}) + \frac{1}{4}F_{aX}(2h_s - h_{s+1} - h_{s-1})\right] \quad (19)$$

where $\tau_o \equiv b(T - T_C^{(o)})$.

Equations 15 and 19 are the constitutive relationships of our theory. Letting $H(x, y) \equiv \cos(q_x x)\cos(q_y y)$, their general solutions are

$$\Phi_s = Ae^{\omega t}H(x,y)e^{iq_z(L+a)s} \quad (20a)$$

$$h_s = Be^{\omega t}H(x,y)e^{iq_z(L+a)s} \quad (20b)$$

where $L + a$ is the lamellar repeat distance. Inserting eqs 20a and 20b into eqs 15 and 19 yields

$$B\left(K_M q^4 + 2F_{aa}\sin^2\left(\frac{1}{2}\hat{q}_z\right)\right) + AF_{aX}\cos^2\left(\frac{1}{2}\hat{q}_z\right) = 0 \quad (21a)$$

$$A\left(\omega + Mq^2\left(\kappa q^2 + \tau_o + F_{XX}\left(\frac{1}{2} - \sin^2\left(\frac{1}{2}\hat{q}_z\right)\right)\right)\right) + BMF_{aX}q^2\sin^2\left(\frac{1}{2}\hat{q}_z\right) = 0 \quad (21b)$$

with $q^2 \equiv q_x^2 + q_y^2$. Because $q_z = \pi s/N(a + L)$, where N is the number of lamellae and $1 \le s \le N$ is an integer, the product $q_z(L + a) \equiv \hat{q}_z$ in eq 21a is independent of the lamellar distance a. The linear algebraic equation (eq 21a) has a nontrivial solution when the determinant of the coefficients of A and B is zero. By imposing such a condition, we find, after a little algebra, the searched dispersion relationship for the fluctuations decay ($\omega < 0$) or growth ($\omega > 0$) is

$$\omega \equiv \omega(\hat{q}_z, q) = -Mq^2[(\kappa q^2 + \tau_o) + \xi(\hat{q}_z, q, a)] \quad (22)$$

κ and τ_o are parameters that depend on the properties of a single isolated bilayer, whereas the function

$$\xi(\hat{q}_z, q, a) \equiv F_{XX}\left(\frac{1}{2} - \sin^2\left(\frac{1}{2}\hat{q}_z\right)\right) - F_{aX}{}^2\frac{\sin^2\left(\frac{1}{2}\hat{q}_z\right)\cos^2\left(\frac{1}{2}\hat{q}_z\right)}{K_M q^4 + 2F_{aa}\sin^2\left(\frac{1}{2}\hat{q}_z\right)} \quad (23)$$

accounts for all of the interbilayer interactions. In the following section, we will discuss the consequences of this important result in determining the onset and evolution of patterns in an array of multicomponent lamellae.

3. Theoretical Results

Isolated Lamellae. Let us first investigate the behavior of the dispersion relationship (eq 22) of an isolated lipid bilayer. In that case $\xi(\hat{q}_z, q, a) = 0$, so eq 22 reduces to the well-known relationship for the spinodal decomposition of a two-component fluid mixture.[1]

$$\omega_o = -Mq^2[\kappa q^2 + \tau_o] \quad (24)$$

Two different scenarios may be envisaged depending on the sign of τ_o. When $\tau_o > 0$, the composition fluctuations, generated by

(22) Smirnov, V. *Cours de Mathematiques Superieures*; MIR: Moscow, 1975; Vol. *IV*

a sudden disturbance of any relevant physical variable, exponentially decay, whereas when $\tau_o < 0$, the fluctuations grow in intensity with time until a macroscopic phase separation occurs. Not all of the fluctuations, however, grow at the same rate. According to eq 24, the fastest growing fluctuation is that satisfying the condition $\partial\omega_o/\partial q = 0$. From the relationship (eq 24), we may calculate the most likely wavevector q_{MAX} (related to the average lateral size of the aggregates: $\langle l \rangle \propto 1/q_{MAX}$) and the so-called "amplification factor", which is the highest growing rate of the fluctuations, calculated at $q = q_{MAX}$

$$q_{MAX} = (-\tau_o/2\kappa)^{1/2} \tag{25a}$$

$$\omega_o^{MAX} = M(\tau_o^2/4\kappa) \tag{25b}$$

From eq 25b, we can also estimate the critical melting temperature of the aggregates by setting $\omega_o^{MAX} = 0$ and solving for T.

Concentrated Lamellae. When we introduce the interactions among the lamellae, the dispersion relationship (22) shows interesting features. To simplify the analysis, let us first consider the simple case of rigid membranes.

Rigid Membranes. ($K_M \rightarrow \infty$). When the bilayer bending rigidity is very large, the last term on the right-hand side of eq 23 vanishes, and the amplification factor reduces to

$$\omega^{MAX} = \frac{M}{4\kappa}\left(\tau_o + F_{XX}\left(\frac{1}{2} - \sin^2\left(\frac{1}{2}\hat{q}_z\right)\right)\right)^2 \tag{26}$$

Recalling that, in isolated lamellae, domains appear when $\tau_o < 0$, we separately consider the cases $F_{XX} < 0$ and $F_{XX} > 0$, where the interbilayer interaction parameter $F_{XX} \equiv \rho\partial^2 F/\partial X^2 = 2\rho(G_{AA}(a) + G_{BB}(a) - 2G_{AB}(a))$ has been calculated from eq 9. (See section 4 for details.) When $F_{XX} < 0$, the amplification factor ω^{MAX} reaches a maximum at $\hat{q}_z \rightarrow 0$, remaining smaller for any other value of $\hat{q}_z$. On the contrary, when $F_{XX} > 0$, the greatest amplification factor ω^{MAX} occurs when $\hat{q}_z \rightarrow \pi$. At both of these extrema, the amplification factor is $\omega^{MAX} = (M)/(4\kappa)(\tau_o - {}^1/_2|F_{XX}|)^2$. The parameter F_{XX} can be modulated by varying the lamellar spacing a, turning, in some cases, from positive to negative.

The physical outcomes of our model are (a) the domains are arranged in-phase or out-of-phase along the z axis, depending on the sign of F_{XX}; (b) the intermembrane interactions always favor the stability of the microdomains (as also evidenced by their higher melting temperature); (c) in a similar way, the interbilayer forces also modify the size of the aggregates, which are always larger than those formed in isolated lamellae; (d) last, there are no unstable fluctuations of the interlamellar distance, with the bilayers remaining flat and with a constant spacing throughout the whole sample. This latter result arises because the amplitude B of the distance fluctuations and that of the composition fluctuations A are related to each other by

$$B = -F_{aX}\frac{\cos^2\left(\frac{1}{2}\hat{q}_z\right)}{K_M q^4 + 2F_{aa}\sin^2\left(\frac{1}{2}\hat{q}_z\right)}A \tag{27}$$

Clearly, B vanishes in the high-rigidity limit of $K_M \rightarrow \infty$.

Soft Membranes. A different scenario arises when the membrane bending rigidity K_M is small but nonzero. The dispersion relationship (eq 22) can be arranged as the sum of three different functions depending on wavevectors q and $\hat{q}_z$

$$\omega = A_1(q) + A_2(\hat{q}_z, q) + A_3(\hat{q}_z, q) \tag{28}$$

Their combination may produce distinct maxima. The first maximum comes out of the term $A_2(\hat{q}_z,q) \equiv -Mq^2F_{XX}({}^1/_2 - \sin^2({}^1/_2\hat{q}_z))$, which occurs at $\hat{q}_z = 0$ ($F_{XX} < 0$) or $\hat{q}_z = \pi$ ($F_{XX} > 0$). Another maximum in the region $0 < \hat{q}_z < \pi$ may arise from the third term of eq 28 ($A_3(\hat{q}_z, q) \equiv Mq^2F_{aX}{}^2(\sin{}^2({}^1/_2\hat{q}_z)\cos^2({}^1/_2\hat{q}_z))/(K_Mq^4 + 2F_{aa}\sin^2({}^1/_2\hat{q}_z))$). It is worth noting that only this latter maximum is responsible for the anomalous multiple periodicity in an array of flexible lamellae. Indeed, when $\hat{q}_z = 0$ all of the lamellae fluctuate in phase, their relative distance remaining constant, whereas in the opposite limit, $\hat{q}_z = \pi$, lamellae fluctuate out of phase, changing their relative distance (Figure 3B). However, such a picture is partially wrong. According to eq 27, the amplitude of the interlamellar spacing fluctuations decreases on increasing $\hat{q}_z$, eventually vanishing at $\hat{q}_z = \pi$. Therefore, the undulated state of Figure 3B, formed by microdomains with alternating smaller and wider spacing, albeit formally allowed, should not be experimentally detectable because of the extremely small intensity of the distance fluctuations. Furthermore, the diffraction patterns associated with the arrangement of Figure 3B also cannot reproduce the typical Bragg line splitting experimentally found in our neutron diffraction measurements. In practice, the only chance to observe Bragg line splitting occurs when the amplification factor has a maximum in the region $0 < \hat{q}_z < \pi$ leading to distorted nonplanar structures such as those in Figure 3A.

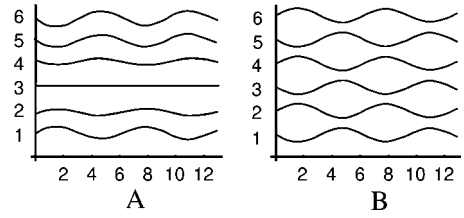

Figure 3. Profile of the interlamellar spacing for two different values of dimensionless wavevector $\hat{q}_z$ perpendicular to the membrane. (A) $\hat{q}_z = 0.5$ and (B) $\hat{q}_z = \pi$. The amplitude of the spacing fluctuations are not in scale; the greater amplitude occurs at lower $\hat{q}_z$ values (A), whereas at $\hat{q}_z = \pi$ (B) the amplitude of the spacing fluctuations is vanishingly small. The lipids are not uniformly distributed, but the less repelling ones accumulate in the short-distance interlamellar regions.

Conditions for the appearance of these local patterns are not easily met. A close inspection of the dispersion relationship (eq 28) shows that the term $A_2(\hat{q}_z, q)$ (responsible for the apparent maxima at $\hat{q}_z = 0$ and π) is generally much greater than the term $A_3(\hat{q}_z, q)$ (responsible for the true maximum at $0 < \hat{q}_z < \pi$). However, when $F_{XX} \rightarrow 0$, the term $A_2(\hat{q}_z, q)$ disappears whereas $A_3(\hat{q}_z, q)$ dominates, ensuring the presence of a true maximum in the region $0 < \hat{q}_z < \pi$. It is interesting to investigate when the condition $F_{XX} \rightarrow 0$ is fulfilled in real systems. (a) Naively, one may conjecture that this condition is met in ideal mixing systems where all of the A−A, B−B, and A−B interactions are identical. However, in the ideal mixing case $A_3(\hat{q}_z, q)$ also vanishes, and the maximum disappears. This means that the interlamellar spacing remains constant even in the presence of compositional microdomains. (b) A more interesting situation occurs in nonideal mixing systems where the j−j' pair interaction shows a different decay length with the interlamellar distance. In this case, F_{XX} changes from negative to positive at some distance. Near this turning point, $F_{XX} = 0$, we have $A_2(\hat{q}_z, q) = 0$, so the dominant contribution to the amplification factor is $A_3(\hat{q}_z, q)$. Physically, the condition $F_{XX} = 0$ is realized in systems with a strong difference in the head group size accompanied by a partial interpenetration of the heads. This peculiar structure of the lipids polar region ensures strong nonideal mixing but avoids an exceedingly high repulsion at short distance. (c) Lastly, multiperiodic structures are very sensitive to the bilayer bending elasticity K_M and to the lateral size $l \approx q^{-1}$ of the compositional

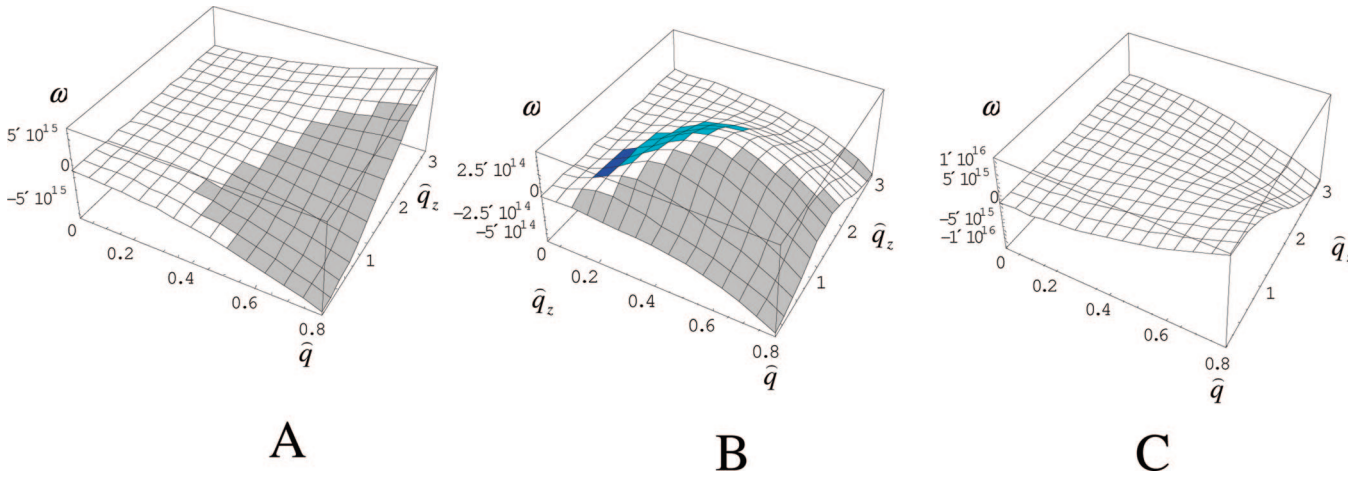

Figure 4. Plot of the amplification factor ω against the parallel ($\hat{q} \equiv q/\sqrt{\rho}$) and perpendicular ($\hat{q}_z$) dimensionless wavevectors with respect to the membrane plane. Plots A−C have been obtained at three different interlamellar distances: (A) $a = 30 \times 10^{-8}$ cm, (B) $a = 20 \times 10^{-8}$ cm, and (C) $a = 10 \times 10^{-8}$ cm. Other parameters are $\rho\Delta_{AA} = 3.5 \times 10^2$ erg·cm^{-2}, $\rho\Delta_{BB} = 4.5 \times 10^2$ erg·cm^{-2}, $\rho\Delta_{AB} = 5.0 \times 10^2$ erg·cm^{-2}, $\lambda_{AA} = 0.020 \times 10^8$ cm^{-1}, $\lambda_{BB} = 0.010 \times 10^8$ cm^{-1}, $\lambda_{AB} = 0.025 \times 10^8$ cm^{-1}, and $X = 0.8$. The remaining parameters are those reported in the numerical calculations section.

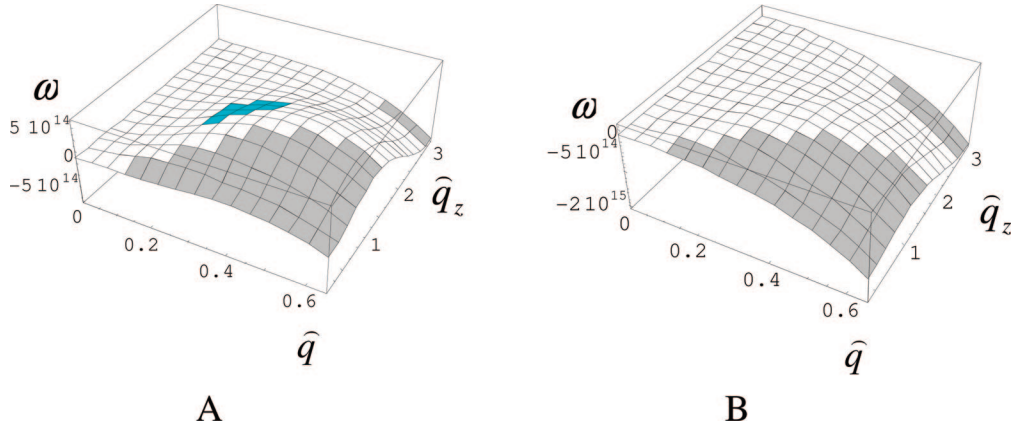

Figure 5. Temperature effect. Plot of the amplification factor ω against the parallel ($\hat{q} \equiv q/\sqrt{\rho}$) and perpendicular ($\hat{q}_z$) dimensionless wavevectors. Plots have been obtained at (A) $T = 273$ K and (B) 350 K, with an interlamellar spacing of $a = 20 \times 10^{-8}$ cm. Other parameters are the same as in Figure 4.

domains. It can be easily shown from eq 28 that, near $F_{XX} \to 0$, the most likely perpendicular modulation of the interlamellar spacing behaves as

$$\hat{q}_z^{MAX} = 2\arcsin\left[-\sigma + \sqrt{\sigma + \sigma^2}\right]^{1/2} \approx \begin{cases} \pi - 2\sqrt{\sigma} & \sigma \ll 1 \\ 1/\sqrt{2\sigma} & \sigma \gg 1 \end{cases} \tag{29}$$

where $\sigma \equiv K_M q^4/2F_{aa}$. As mentioned before, the amplitude of the anomalous lamellar spacing is vanishingly small both at $\hat{q}_z^{MAX} = 0$ and π; therefore, according to eq 29, perpendicular domains disappear either when $\sigma \gg 1$ (infinitely rigid membranes, $K_M \to \infty$) or when $\sigma \ll 1$ (very large lateral domains, $q \to 0$). It is worth mentioning that the addition of bulky impurities to lipid bilayers generally leads to an overall membrane softening.[23−26]

Typical results are shown in Figure 4, where we report the amplification factor ω against the dimensionless parallel ($\hat{q} \equiv q/\sqrt{\rho}$) and perpendicular ($\hat{q}_z$) wavevectors. We considered a nonideal mixture of two lipids where the A−B repulsions are stronger than the average A−A and B−B ones, but the decay of the A−B interactions with the interlamellar distance is faster. In such a system, domains are favored at short distance and disfavored at large distance. When $F_{XX} \neq 0$, the highest amplification of the spacing fluctuation occurs at $\hat{q}_z = 0$ or π (panels A and C). However, near the turning point, $F_{XX} \to 0$, the onset of large domains with different spacing is extremely likely, as evidenced by the onset of a net maximum in the region $0 < \hat{q}_z < \pi$ (panel B). In our simulation, the tuning of the nonideal mixing parameter F_{XX} is performed by varying the interlamellar distance a through the amphiphile/water ratio. It can be easily seen that there is an optimum distance at which large domains with an anomalously large interlamellar distance can be easily formed. At shorter or higher distances, these domains may either dissolve or retain a different composition while assuming a constant interlamellar spacing. Several parameters can be varied, other than the distance. For instance, high temperatures may lead to domain dissolution, as shown in Figure 5. Here, the effect of even modest heating is clearly evidenced by the disappearance of the maximum in the amplification factor.

The linearized spinodal decomposition theory that we have developed captures just the first events of the phase separation

(23) Fosnaric, M.; Iglic, A.; May, S. *Phys. Rev. E* **2006**, *74*, 051503.
(24) Bivas, I.; Meleard, P. *Phys. Rev. E* **2003**, *67*, 012901.
(25) Brocca, P.; Cantù, L.; Corti, M.; Del Favero, E. *Prog. Colloid Polym. Sci.* **2000**, *115*, 181.
(26) Brocca, P.; Cantù, L.; Corti, M.; Del Favero, E.; Motta, S. *Langmuir* **2004**, *20*, 2141.

in a cluster of multicomponent interacting lamellae. The final morphology of the sample, however, keeps track of the first events, but it may further evolve into rather different structures. These ripening processes are even more likely in the studied case because of the presence of two different time scales (fast lateral lipid motion and slow interlamellar lipid transfer). In its present development, the model predicts the formation of localized deformed patches inside an array of lamellae. These distorted patches appear in the early stages of the phase-separation process and are favored by specific intermolecular interactions among the lipid heads, but they are hampered by the bilayers' bending deformation energy. On slowly approaching thermodynamic equilibrium, the lipid exchange allows for the formation of lamellae richer in the A or B component, eventually leading to a macroscopic phase separation where tightly packed and swollen lamellae coexist.[17,18]

4. Numerical Calculations

Numerical results were obtained by using the following parameters: the bending elasticity modulus $K_M = 0.4 \times 10^{-12}$ erg $\approx 10kT$, the thermal energy $kT \approx 0.4 \times 10^{-13}$ erg at $T =$ 273 K, the 2D membrane density $\rho = 2 \times 10^{14}$ cm^{-2}, the fraction of B lipids in an A + B mixture with $X = 0.2$, and the nonideal mixing parameter $w/kT = 2.5$. The lamella−lamella interaction energy per unit surface F was estimated from the pairwise additivity rule (eq 9). Here the interaction energy among the $j-j'$ pairs has been described by the trial function $G_{jj'}(a) = \Delta_{jj'}e^{-\lambda_{jj'}a}$ commonly used to reproduce the behavior of electrostatic and hydration forces in membranes, with the constants $\Delta_{jj'}$ and $\lambda_{jj'}$ being a measure of the strength and decay of the intermolecular repulsion, respectively. At short distances, the overwhelming contribution to the interlamellar energy comes out of the hydration forces. At physiological salt concentration and room temperature, the electrostatic contribution turns out to be about 10−20% of the hydration forces, even at high surface potentials, whereas dispersion forces are even smaller. Typical values are $\rho\Delta_{jj} \approx 10^2$ erg·cm^{-2} and $\lambda_{jj} \approx 2 \times 10^{-8}$ cm.[27]

5. Materials and Methods

DMPC (1,2-dimyristoyl-*sn*-glycero-3-phosphatidylcholine) and C16-sphingomyelin (*N*-palmitoyl-D-erythro-sphingosylphosphorylcholine), called SM in the following text, were purchased from Avanti Polar Lipids. Appropriate amounts were first dissolved in chloroform. GM1, extracted and purified as described in ref 28 and obtained as a sodium salt powder, was dissolved in chloroform/methanol 2:1 to be used for mixed sample preparation. If necessary, compounds were admixed while dissolved in an organic solvent. Highly oriented multistacks of pure DMPC and mixed DMPC/SM = 96:4 mol (DMPC/SM hereof) and DMPC/GM1 = 97:3 mol (DMPC/GM1 hereof) were obtained as follows. Lipid films were prepared in vials starting from solutions of about 20 mg/mL by carefully evaporating the organic solvent and then drying with a water pump for 1 h. The lipid films were then dissolved in D_2O (20 mg/mL) and subjected to sequential cycles of freezing and thawing, according to a well-assessed protocol, to obtain good homogeneity. The D_2O solutions were then spread on silicon wafers and dehydrated in the oven at 40 °C for 24 h. Samples were then kept in D_2O-saturated air for 72 h before measurement.

Measurements were performed at the Institut Laue Langevin (ILL), France on the instrument D16[29] using a vertically focused neutron beam of wavelength 4.53 Å with a 1% spread, fwhm. The area detector (256 × 256 mm^2, 2 mm resolution) was seated on a radial arm of a circular track centered at the sample. Measurements were carried out with a detector−sample distance of 1 m. The samples were kept in a temperature- and humidity-controlled chamber, monitored by two sensors positioned close to the sample.[30] To acquire data, the samples were first aligned by using a pseudo $\theta/2\theta$ configuration, made by fixing the position of a 2D detector and scanning the sample by 0.2° around the first Bragg peak of the multilayer films. Acquisitions were made by keeping both the detector angle and the sample angle at a position such that the Bragg peaks were centered on the detector. The 2D images were integrated and plotted versus q_z, the scattering vector perpendicular to the membrane stacks ($q = 4\pi/\lambda \sin\theta$). The resolution of q_z was about 0.0025 Å. The typical exposure time was 100 s in the low-q region and 900 s in the high-q region.

6. Experimental Results

The experiment was designed in order to verify the effect of in-membrane 2D clustering on the 3D organization of a multistack of lamellae composed of mixed lipids. The organization of the multistack in the direction normal to the stack is reflected in the interlamellar repetition distance that gives rise to a Bragg peak in q space. The lipid mixture, based on DMPC, was selected so as to enhance the consequence of in-membrane defect formation (clusterization) on the stacking of adjacent membranes. Thus, a bulky headgroup and a long-ceramide-chain amphiphilic molecule, namely, GM1 ganglioside shown in Figure 2, were chosen as the second lipid to be mixed with the DMPC phospholipid in a low proportion (3% mol), very far from the half-mole fraction. The nonhomogeneity of lipid chains induces in-membrane segregation of the two lipids, which can be amplified by the huge difference in headgroup size of DMPC and GM1. Because of the complexity of GM1 headgroups consisting of four neutral sugars plus a charged one, sialic acid, a complex set of interactions occurs on the lamellar surface, including steric, electrostatic, hydration, and preferential interactions between similar lipids. In the lamellar phase, this may results in pair interactions between j and j' molecules sitting on adjacent bilayers, showing different spatial decays, as required by the model described above and then governing the molecular distribution at different interlayer distances. The presence of a spontaneous cluster of GM1 molecules, with their headgroups protruding out of the bilayer, constitutes a cross defect for the multistack. Therefore, DMPC/GM1 multistacks at low hydration are good candidates for studying the 2D-domain-induced 3D effect in ordered arrays of mixed lamellae.

As a possible counterexample, DMPC was also mixed with sphingomyelin (SM), again in a low mole ratio, and a multistack system of a mixed DMPC/SM lamellae was investigated. In fact, as shown in Figure 2, SM bears the long ceramide chains that can induce in-membrane segregation, but the same small phosphocholine headgroup of DMPC. Thus, SM should not display any preferential interactions among facing headgroups.

Figure 6 shows small angle (panel A) and wide angle (panel B) neutron diffraction spectra from membrane multistacks in the gel phase, at 20 °C, for the three investigated systems: pure DMPC, mixed DMPC/SM (96:4 mol %), and mixed DMPC/GM1 (97:3 mol %). The single intense peak of the Bragg first repetition line in the small-angle range corresponds to an interlamellar distance of 54.4 Å for pure DMPC (as expected for the L_c phase under dehydrated conditions[31]) and 54.3 Å for a mixed DMPC/SM stack. However, the mixed DMPC/GM1

(27) Rand, P.; Parsegian, V. A. *Biochim. Biophys. Acta* **1989**, *988*, 351.
(28) Tettamanti, G.; Bonali, F.; Marchesini, S.; Zambotti, V. *Biochim. Biophys. Acta* **1973**, *296*, 160.
(29) Leonard, A.; Escrive, C.; Laguerre, M.; Pebay-Peyroula, E.; Neri, W.; Pott, T.; Katsaras, J.; Dufourc, E. J. *Langmuir* **2001**, *17*, 2019.
(30) Perino-Gallice, L.; Fragneto, G.; Mennicke, U.; Salditt, T.; Rieutord, F. *Eur. Phys. J.* **2002**, *E 8*, 275.
(31) Foster, G.; Meister, A.; Blume, A. *Curr. Opin. Colloid Interface Sci.* **2001**, *6*, 294.

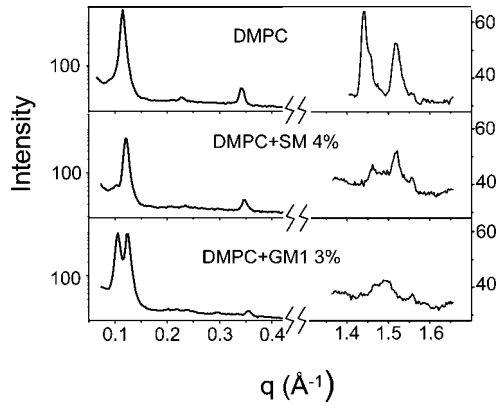

Figure 6. Neutron diffraction experiments of lamellar multistacks of single-component DMPC, mixed DMPC/SM (96:4 mol), and DMPC/GM1 (97:3 mol) at 20 °C in the gel phase. Small angle (left): Bragg peaks corresponding to interlamellar repetition distances. Wide angle (right): spectra in the region of the chains' nearest-neighbor correlation peak. In the case of the DMPC/GM1 mixed system, interlamellar Bragg first repetition splits and definitive chain order loss are observed.

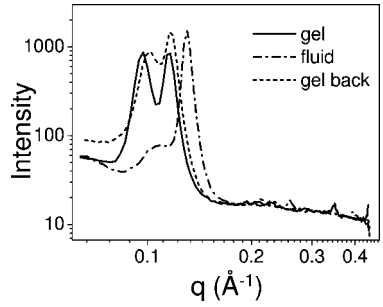

Figure 7. SA neutron spectra of DMPC/GM1 in the gel phase at 20 °C (—), in the fluid phase at 54 °C (-•-), and back at 20 °C (---). In the fluid phase, the Bragg peaks merge into a single line.

spectrum shows two Bragg lines corresponding to interlamellar distances of 54.3 and 65.1 Å. The lamellar second repetitions are faint because of convolution with the lamella form factor. Panel B of Figure 6 reports the wide-angle spectra detailing the local order of the lipid chains. The two observed peaks of DMPC are characteristic of the orthorhombic symmetry of the chain order in the L_c phase in the q range corresponding to the 4 Å interchain distance. The degree of local order is lowered in the mixed DMPC/SM system and almost suppressed in the case of DMPC/GM1. This indicates that both SM and GM1 intimately mix with DMPC within each lamella. This result is decisive in the case of DMPC/GM1 since no residual pure-DMPC signal is observed, eliminating the hypothesis of macroscopic phase separation being at the basis of the observed double repetition in the multistack cross direction. In the present case, local bunches with anomalous spacing are spread within the multistack. The behavior of DMPC:SM multistack is different, maintaining a single interlayer distance, slightly lower than pure DMPC. Because of the similar structure of the polar region, the mixing behavior of the headgroups of DMPC and SM is not affected by any preferential interaction (namely $\xi(\hat{q}_z,q,a) = 0$ in eq 22)). In such a case, the existence of multiple interlayer distances is forbidden even in the presence of compositional microdomains induced by the nonideal mixing of the hydrocarbon tails.

Figure 7 shows small-angle neutron diffraction results obtained for the mixed DMPC/GM1 multistack as a function of temperature. By heating the sample above the melting temperature, at 56 °C, the Bragg peak splitting disappears, and a single peak is observed corresponding to an interlamellar distance of 48.3 Å. A similar reduction is expected for a stack of phospholipid bilayers going from the gel to the fluid L_α phase. A temperature scan back to 20 °C results in the resplitting of the Bragg line into two peaks at same positions as the initial ones, indicating full reversibility of the bunched lamellar stacking. The temperature behavior reported in Figure 7 is consistent with the theoretical results of Figure 5. They show the disappearance of multiple interlayer distances with temperature, as evidenced by the lowering of the maximum of the amplification factor $\omega(q, \hat{q}_z)$ in the region $0 < \hat{q}_z < \pi$. We want to stress that the disappearance of multiple interlayer distances above the chain-melting transition temperature does not imply dissolution of the clusters. They may still exist (provided ω has a maximum at some q), but the lipid layers remain basically flat.

7. Conclusions

We developed a model for local phase separation in lamellar multistacks of mixed lipids with different packing requirements, accounting for the existence, at short times, of finite bunches with nonaverage interlamellar distances. While driving over long times to macroscopic phase separation, requiring interlamellar molecular transfer, local phase separation occurs at short times when only intralamellar diffusion can take place. For soft mixed membranes, the bending energy cost for distorting each lamella within the bunch from the flat configuration is overrun by preferential interactions among similar lipids. In-plane clustering can be reproduced in few in-phase replicas rather than dissipated by molecular rediffusion, when pair molecular interactions show different spatial decays with the interlamellar distance. As shown in the Experimental Results section, this is the case for multistacks of deformable mixed lamellae of phosphatidylcholines and gangliosides, where huge differences in packing favors clustering and partial head interpenetration avoids an exceedingly high repulsion at short distance.

This short-time behavior is of particular interest if related to real membranes. In fact, it predicts the stabilization against lipid redistribution of similar domains sitting on different membranes coming into contact at short times. It is has been claimed that glycosphingolipid-enriched microdomains interfacing between two adjacent cells mediate important physiological processes as cell-to-cell adhesion.[32] The proposed model sketches in simple terms the possible local structural response to a domain−domain interaction taking place between close-facing membranes before specific physical and biological events take place.

LA802858M

(32) Hakomori, S. *Proc. Jpn. Acad.* **2005**, *81*, 189.